MALAYSIAN JOURNAL OF ANALYTICAL SCIENCES

Journal homepage: https://mjas.analis.com.my/

Research Article

In silico characterization of low silica inducible influx transporter proteins in rice plant, *Oryza sativa* towards silicic acid nanoparticles

Nik Nur Syafiqah Zaini Safayi, Aziz Ahmad, Siti Aisyah Razali, Muhamad Fairus Noor Hassim*

Special Interest Group Modelling and Data Analytics (SIGMDA), Faculty of Science and Marine Environment, Universiti Malaysia Terengganu, Kuala Nerus, Terengganu, Malaysia 21030

*Corresponding author: muhamad.fairus@umt.edu.my

Received: 17 December 2025; Revised: 16 June 2026; Accepted: 24 June 2026; Published: 31 October 2026

Abstract

Silica nanoparticles (SiNPs) derived from recycled agricultural waste have shown potential to enhance crop productivity, particularly in rice (*Oryza sativa*), where silica uptake is mediated by the Low-Silicon transporter proteins LSI1 and LSI6. However, the molecular interaction between SiNPs and these transporters remains poorly understood. This study used an in-silico approach to elucidate the interaction between ortho-silicic acid ($Si(OH)_4$), a hydrated form of silica, and LSI1 and LSI6. Three-dimensional protein structures were retrieved from RCSB PDB, AlphaFold, Robetta, and Swiss-Model, while the ligand structure was obtained from PubChem. Active binding sites were analyzed using FTsite and Clustal Omega. Molecular docking was performed using AutoDock Vina, and the results were visualized with Biovia Discovery Studio. Primary structure analysis identified the conserved asparagine-proline-alanine (NPA) motif in both LSI1 and LSI6. Tertiary structure modeling revealed three channel-like binding sites in each protein. Docking analysis indicated hydrogen bonding and van der Waals interactions, with binding affinities of -3.8 kcal mol^{-1} (LSI1) and -4.0 kcal mol^{-1} (LSI6), involving key residues such as glycine, serine, and arginine. The findings suggest transient yet consistent interactions, supporting the hypothesis of a regulated, rapid silica-uptake mechanism in rice plants.

Keywords: In silico docking, LSI1 and LSI6, ortho-silicic acid, rice transporter protein, transporter protein interaction

Introduction

Climate change, characterized by significant long-term alterations in average climate conditions, poses a major threat to plant sustainability and global food security [1]. One of its critical consequences is drought, which causes water scarcity, harms human populations, and reduces agricultural productivity, including that of rice (*Oryza sativa*), a staple in Malaysia. Compared with crops such as wheat, maize, and sorghum, rice is more drought-sensitive because of its greater water dependence throughout its life cycle [2]. Arid environments can significantly inhibit plant growth and biochemical activity [3, 4]. As drought intensifies under climate change and pressure mounts to improve rice production under limited water availability, silica nanoparticle (SiNPs)-based approaches are attracting growing attention as a potential sustainable strategy in agriculture. However, the molecular mechanisms underlying silica uptake in rice, particularly those involving transport proteins, remain poorly understood and warrant further study.

Currently, Malaysia's Self-Sufficiency Level (SSL) for rice is 63% and is targeted to reach 75% in the coming years, according to NAP 2.0. Therefore, innovative strategies are required to improve rice production, as rice remains a staple for a large proportion of the global population. Silica nanoparticles (SiNPs) have been widely reported to enhance rice plant growth and grain yield [5, 6]. Although silicon (Si) is not an essential element for plants, it is still considered advantageous for some crops [7–9].

Previous studies have shown that SiNPs enhance plant resistance to both biotic and abiotic stresses [10-15]. For example, drought-stressed rice treated with SiNPs exhibited higher grain yield and proline content than untreated plants [12]. Root-applied SiNPs improve root development under water-limited conditions, enabling plants to access deeper soil moisture [13]. SiNPs also alleviate salt stress in pea plants and drought stress in wheat [14, 15]. In soil, silica nanoparticles dissolve into ortho-silicic acid ($Si(OH)_4$), which is absorbed by plant roots and transported to shoots, where it polymerizes into

hydrated amorphous silica, reinforcing cell walls and providing structural strength. In rice, transport of $Si(OH)_4$ is mediated by specific transporter proteins: LSI1 and LSI6 (influx) and LSI2 and LSI3 (efflux) [16].

Molecular docking is a computational approach used to predict and analyze interactions between proteins and ligands [17]. This study predicts the optimal ligand-protein binding mode and generates a range of potential ligand orientations within the target protein's binding site [18]. Although previous studies have primarily focused on LSI1 due to its resolved crystal structure and well-characterized silica-selective filter [19–21], limited information is available on its homolog, LSI6. This study focuses on docking-based prediction as the main in silico screening approach to explore interactions between $Si(OH)_4$ and rice silicon transporters. A comparative analysis of binding affinities and interaction patterns was conducted to enhance understanding of the silica transport mechanism mediated by these influx proteins in rice.

Materials and Methods

Structural analysis of transporter proteins is essential in molecular research because it provides key insights into their functional properties. Additionally, understanding the interactions and roles of the protein with a target ligand can improve productivity and plant resilience to various stresses [22]. In this study, the sequence and structure of the LSI6 transporter protein were characterized using models generated from multiple sources. A computational approach was employed to predict binding sites and investigate interactions between silica nanoparticles (SiNPs) and all LSI transporter proteins in rice using molecular docking analysis (**Figure 1**).

Protein analysis

The software and databases used in this study are summarized in **Table 1**. A primary sequence alignment between the reference protein LSI1 and the predicted LSI6 protein was performed using the Clustal Omega online tool. The Expasy ProtParam tool was used to determine the proteins' physicochemical properties and amino acid composition. Because no crystal structure for LSI6 was available, multiple three-dimensional (3D) models were generated from the FASTA sequences using structure-prediction servers such as AlphaFold, Robetta, and Swiss-Model. The crystal structure of the reference LSI1 protein (a homotetramer) was retrieved from the RCSB Protein Data Bank (PDB ID: 7CJS), and the 3D structure of ortho-silicic acid ($Si(OH)_4$) was obtained from PubChem (CID: 14942).

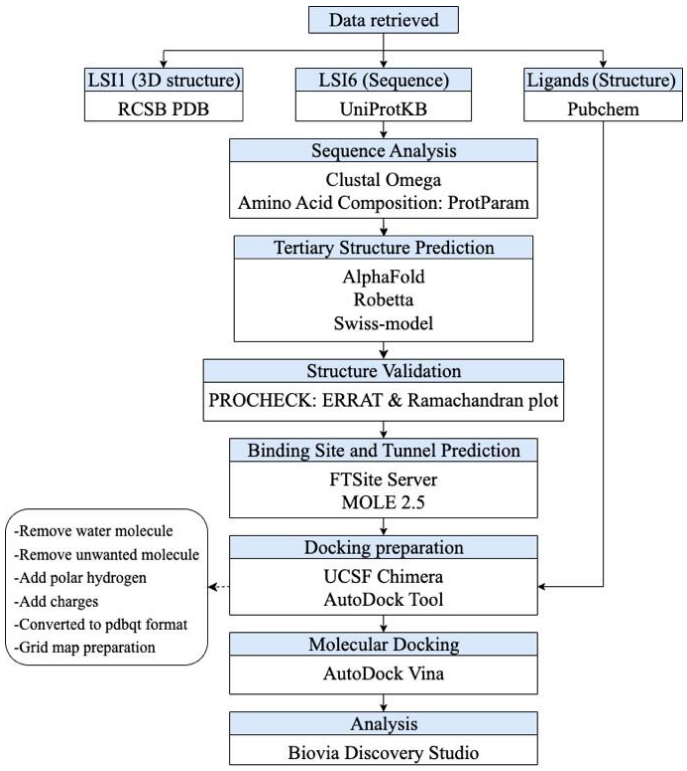


Figure 1. Experimental design for the study of the interaction between $Si(OH)_4$ and predicted LSI6 transporter proteins.

Table 1. List of programs and databases used in the molecular docking study, with citations and links

		Citation	Link
Programs	Clustal Omega	[25]	https://www.ebi.ac.uk/jdispatcher/msa/clustalo
	ProtParam	[26]	https://web.expasy.org/protparam/
	FT Site	[27]	https://ftsite.bu.edu/
	PyMOL 2.5.2	[28]	https://pymol.org/2/
	MOLE 2.5	[29]	https://mole.upol.cz/
	Saves v6.0	[30]	https://saves.mbi.ucla.edu/
	UCSF Chimera	[31]	https://www.cgl.ucsf.edu/chimera/
	Autodock Vina	[31, 32]	https://vina.scripps.edu/
	BIOVIA DS	[33]	https://discover.3ds.com/discovery-studio-visualizer-download
Database	AlphaFold	[34]	https://www.uniprot.org/
	Robetta	[35]	https://robetta.bakerlab.org/
	Swiss Model	[36]	https://swissmodel.expasy.org/interactive
	RCSB PDB	[37]	https://www.rcsb.org/
	UniProtKB	[38]	https://www.uniprot.org/
	PubChem	[39]	https://pubchem.ncbi.nlm.nih.gov/

Structural validation was conducted to assess the reliability of the predicted protein models. Subsequently, all LSI6 models were evaluated using the SAVES v6.0 online server with two key validation tools: ERRAT and the Ramachandran Plot. Models that met the quality thresholds (ERRAT >95% and Ramachandran Plot >90%) were considered structurally sound. The validated LSI6 model with the most favorable scores was selected for further molecular docking analysis [23, 24].

Binding site and tunnel identification

An online server, FTSite Server (http://ftsite.bu.edu), was used to identify the active binding sites of all LSI proteins. This tool also identifies additional binding-site residues and conserved regions, including the Asn-Pro-Ala (NPA) domain motif of the NIP III family (LSI1 and LSI6). Further 3D visual editing and marking of the sequences and domain of interest were conducted using PyMOL 2.5.2 [28]. Similarly, MOLE 2.5 provided a comprehensive list of predicted surface-accessible channels that may accommodate ligand binding [29]. Binding pockets and channels exhibiting tunnel-like characteristics were selected as the predicted binding regions for subsequent molecular docking analysis.

Docking preparation

The selected LSI6 protein models were prepared for docking analysis using the Dock Prep function in UCSF Chimera. This preparation step involved removing non-protein components, such as water molecules and existing ligands. Polar hydrogens were added, and Gasteiger charges were assigned to each structure. Both the proteins and ligands were then converted to the PDBQT format, which is required for docking [40]. Docking coordinates and grid box dimensions were configured based on the previously predicted binding sites, defining the spatial region where ligand docking would occur. These steps were performed throughout the study to ensure consistency and reduce the potential bias.

Molecular docking and analysis between LSI6 and $Si(OH)_4$

Molecular docking simulations between $Si(OH)_4$ and all LSI transporter proteins were performed using AutoDock Vina v1.2.5. Each docking run used an exhaustiveness value of 8, with the default scoring function retained. AutoDock Vina evaluates the binding affinity between a ligand and receptor by predicting their interaction energy. The conformation with the lowest binding energy, indicating the highest binding affinity, was selected for further analysis. Binding affinities were expressed in kcal mol^{-1} [41]. The binding interactions between each LSI transporter protein and $Si(OH)_4$ were visualized using Biovia Discovery Studio [33]. The output shows both three-dimensional (3D) and two-dimensional (2D) intermolecular interactions, including hydrogen bonds and Van der Waals interactions.

Results and Discussion

LSI6 is a homolog of the LSI1 transporter protein, which plays a crucial role in regulating the transport of silicic acid [$Si(OH)_4$] in rice plants. While LSI1 primarily mediates $Si(OH)_4$ influx into root cells, LSI6 performs a similar function in the shoot, specifically in the node I region. LSI6 mediates the distribution of silicic acid toward the panicle, contributing to efficient silica allocation within the plant. Although the physiological effects of silica application in rice have been reported [19], it is also important to investigate the molecular characteristics and mechanisms underlying the interaction between $Si(OH)_4$ and the LSI6 transporter protein.

Primary sequence analysis of LSI6 transporter protein

Primary sequence analysis and verification are pivotal in protein characterization. In this study, the physicochemical properties of LSI6 were obtained using the ExPASy ProtParam online tool. The transporter protein was predicted to have a molecular weight of 23.52 kDa and a theoretical isoelectric point (pI) of 7.12. The normal theoretical pI value indicates that LSI6 is a neutral protein, carrying no net charge at pH 7. This result was supported by a previous study showing that LSI1 also functions as a transmembrane protein. LSI6 also exhibited a very high aliphatic index (105.45), which is associated with long aliphatic side chains, suggesting the protein is stable over a wide range of temperatures [42-44].

On the other hand, a balanced value of the grand average of the hydropathy index (GRAVY, 0.814) was obtained. GRAVY was calculated as the sum of the residue hydropathies divided by the total number of residues in that protein [45]. Previous research also stated that a positive GRAVY value is highly indicative of a hydrophobic membrane-bound protein [46, 47]. In this study, GRAVY values suggested hydrophobic properties and a transmembrane structure for the LSI6 protein. The predicted LSI6 sequence indicates that the protein is predominantly nonpolar, with Valine (Val) the most abundant, followed by Alanine (Ala) and Glycine (Gly) (Figure 2). Meanwhile, in LSI1, Ala is the most abundant amino acid, accompanied by Val and Gly. Furthermore, sequence analysis between LSI1 and LSI6 shows that the LSI6 transporter has a similar sequence identity with LSI1 (80.18%).

Furthermore, the Major Intrinsic Protein (MIP) family includes five subfamilies: Tonoplast (TIP), Nodulin-26 (NIP), Plasma membrane (PIP), Small basic (SIP), and unclassified (XIP). Influx silica transporters belong to the NIP family and share the Asn-Pro-Ala (NPA) motif conserved among aquaporins. Further analysis of the multiple sequence alignment reveals two conserved regions, each three amino acids long, in LSI1 (Asn108, Pro109, Ala110, and Asn219, Pro220, Ala221) and LSI6 (Asn111, Pro112, Ala113, and Asn222, Pro223, Ala224) (Figure 3). According to Table 3**,** the NPA regions in LSI1 and LSI6 are located in the middle of the protein's channel. They form the bottleneck, the narrowest part that allows only water molecules to pass through the channel.

LSI1 and LSI6 are highly selective proteins, as they contain several silica selectivity filter (SF) residues that are also important for distinguishing specific silica transporter proteins from other aquaporins. There are five residues involved in the SF: Thr65, Gly88, Ser207, Gly216, and Arg222 [19, 21]. These amino acids determine a specific channel through which $Si(OH)_4$ molecules can pass. The silica SF residues for LSI6 are similar and align with the SF residues of the LSI1 transporter protein. Thus, these primary sequence analyses support the previous study, which stated that LSI6 is a homolog with characteristics like those of LSI1.

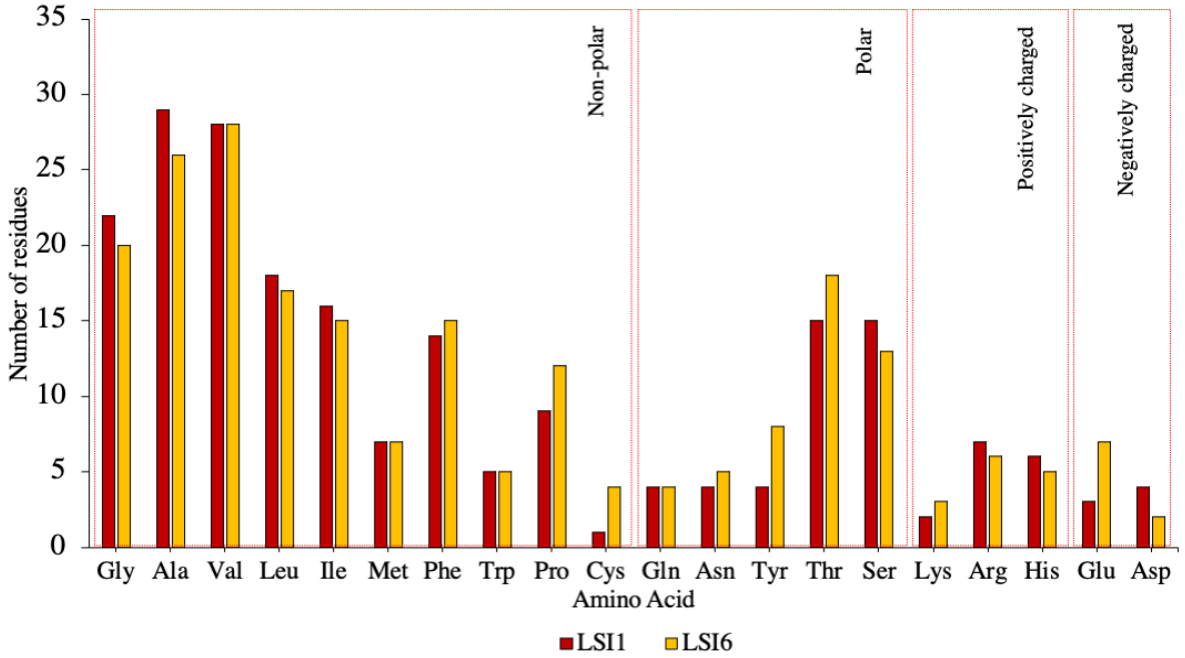


Figure 2. Amino acid composition of the LSI1 (PDB ID: 7CJS) and LSI6 (UniProt ID: Q67WJ8) transporter proteins, obtained from ProtParam. Red dashed box: classification of amino acids



Figure 3. Sequence alignment of the silica influx transporter proteins LSI1 and LSI6. Green letters: Residues predicted to be involved in binding. Red box: NPA domain motif. Triangle: Residue of the silica selectivity filter

Structures validation of LSI6

The three-dimensional (3D) structure of a protein is crucial for understanding its function and properties. Since the crystal structure of LSI6 is unavailable, three predicted 3D structures were generated using AlphaFold, Robetta, and Swiss-Model to increase confidence in the prediction model through comparison. LSI6 is also closely related to the well-characterized LSI1 transporter protein, which serves as a useful homolog for structural and functional reference. AlphaFold, as implemented in the UniProt Knowledgebase (UniProtKB), predicted the LSI6 structure (298 amino acids) with high overall confidence and identified two extended terminal strands [48]. Of the 298 residues, 98 had a per-residue confidence score (pLDDT) below 90, suggesting structural instability [49]. These regions are typically more flexible or less ordered, especially at the termini, and are unlikely to significantly affect the overall protein fold or structural reliability.

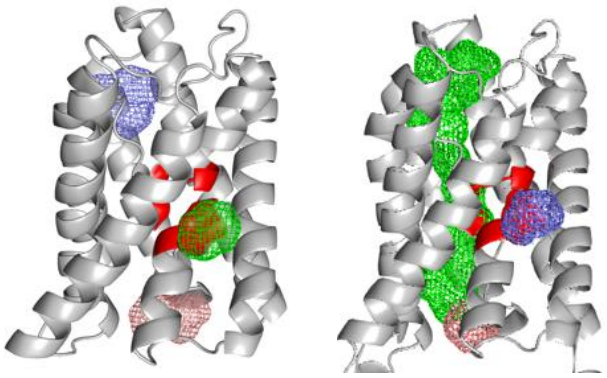
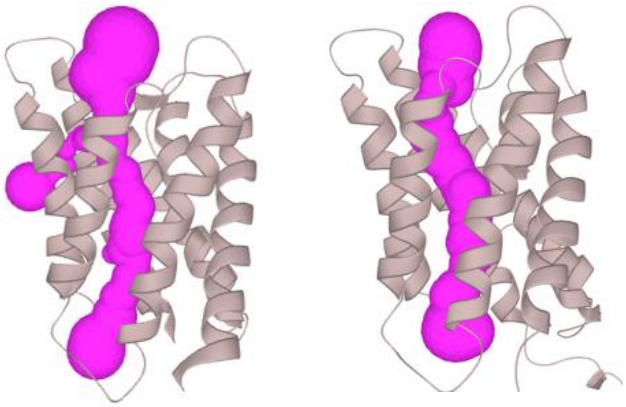
Swiss-Model predicted the quaternary structure of LSI6 using a combination of algorithms, including BLAST and a support vector machine (SVM) [50], suggesting that LSI6 forms a homotetramer composed of four identical subunits. This structure is consistent with the related LSI1 transporter protein. Meanwhile, Robetta, which applies the RoseTTAFold method, predicted a structure with a confidence score of 0.73, indicating good overall structural quality [33]. It also provided an estimated error range (<1 Å to <5 Å) based on CAMEO, indicating the predicted distance between the Cα atoms in the model and those in the native structure. All three models showed high similarity to the LSI1 transporter, providing strong support for the prediction's reliability.

Furthermore, the Ramachandran plot analysis and the ERRAT score were used to evaluate overall model quality based on nonbonded atomic interactions (Table 2). The validation results showed that most predicted structures were highly reliable, with more than 90% of residues in the favored regions of the Ramachandran plot. In addition, the ERRAT score exceeded 90% for all generated structures. Based on these results, although the Robetta model achieved slightly higher validation scores on certain metrics, the AlphaFold model was ultimately selected for further investigation. This decision was based on AlphaFold's algorithm, which has proven highly accurate in subsequent molecular investigations [32]. Overall, this workflow highlights the use of multiple prediction tools and validation techniques to ensure confidence in the selected LSI6 protein model.

Table 2. Validation analysis of the predicted structure of the LSI6 protein; ERRAT Score (%) and Ramachandran Plot (%) using Saves v6.0 software

Protein	Source	Protein Validation	
		ERRAT Score (%)	Ramachandran Plot (%)
LSI6	AlphaFold	95.89	90.30
	Robetta	98.75	90.20
	Swiss-Model*	93.14	90.60

Table 3. Binding site and tunnel predictions for the LSI1 and LSI6 transporter proteins. The colored meshes and the pink surface represent the predicted binding site and potential transport tunnels for Si(OH)4 passage, respectively. The red ribbon highlights the conserved NPA motif, which corresponds to the transporter's bottleneck region

Programs	Protein Models	
	LSI1	LSI6
FTSite		
Mole2.5		

Binding site tunnel and characterization

Identifying binding sites and potential tunnel pathways is crucial for understanding how proteins function as silica transporters in plants. In this study, FTSite was used to predict binding sites, and MOLE 2.5 was used to identify potential tunnel pathways in LSI proteins. Together, these tools provide better insight into ligand binding and its passage through proteins. FTSite has been reported to achieve up to 94% accuracy in identifying the predicted binding site in the apo-protein [51]. In this study, FTSite identified several potential binding sites within the proteins that were most likely to bind silica nanoparticles. In addition, MOLE 2.5 detected internal cavities and channels that could serve as pathways for ligand movement [29].

Overall, the results suggest that several potential binding sites in LSI6 are located in the protein's central region, forming a continuous tunnel-like pathway for ligand passage. This is further supported by structural visualization (**Table 3**), in which FTSite-predicted binding cavities (green meshes) overlap with the tunnel pathway identified by MOLE 2.5 (pink surface) that connects the protein's posterior and anterior regions. This overlap between the two analyses strengthens the idea that these regions are important for ligand binding and transport. In addition, the silica selectivity filter residues overlap with predicted binding sites from molecular docking.

The NPA regions define the bottleneck shape, which represents the narrowest part of the channel (Table 3). This region is located near the conserved Thr-Gly-Ser-Gly-Arg (TGSGR) motif, which serves as the selectivity filter for $Si(OH)_4$ [19]. In LSI1, the selectivity filter residues are $Thr65_{TM1}$, $Gly88_{TM2}$, $Ser207_{TM5}$, $Gly216_{LE1}$ and $Arg222_{LE2}$, whereas in LSI6 they are predicted to be $Thr68_{TM1}$, $Gly91_{TM2}$, $Ser210_{TM5}$, $Gly219_{LE1}$ and $Arg225_{LE2}$. These conserved residues play a critical role in maintaining the pore structure and facilitating the selective movement of silicic acid across the membrane.

In addition, silicon transporter proteins from other plant species are expected to exhibit similar binding interactions with silicic acid due to conservation of key amino acid residues involved in substrate recognition. These conserved residues, particularly those in the aromatic/arginine (ar/R) selectivity filter and NPA motifs, play an important role in silicon transport. Therefore, the silicon transport mechanism is likely to be similar across different plants. Consistent with this, in monocotyledonous plants such as rice, wheat, and maize, the uptake of SiNPs is facilitated by specific silicon transporter proteins, including OsLSI1 (PDB ID: 7CJS), Si2 (UniProt ID: F1SX50), and NIP21_MAIZE (UniProt ID: Q19KC1) [52, 53].

Molecular docking between LSI6 and $Si(OH)_4$

Nine predicted conformations of the LSIs-$Si(OH)_4$ complex were obtained from docking results, and the best binding score (binding affinity) for each was further investigated. Further analysis shows seven hydrogen bonds linking $Si(OH)_4$ and the active binding site of LSI1, with a binding affinity of -3.8 kcal mol^{-1} (**Table 4**). $Si(OH)_4$ is predicted to form four hydrogen bonds with three amino acids: Gly215, Gly216, and Arg222. The interaction also revealed that certain residues stabilize the ligand through Van der Waals interactions. These involve residues Thr65, Ala66, Ala69, Gln84, Ser85, Gly88, Thr157, Ser207, Gly211, and Ser217.

Additionally, the interaction between $Si(OH)_4$ and LSI6, as predicted by the AlphaFold model (UniProt ID: Q67WJ8), yields a binding affinity of -4.0 kcal mol^{-1}. As with LSI1, four hydrogen bonds were observed between the ligand and residues of LSI6, including Gly218, Ser210, and Arg225. For this homolog, Thr68, Ala72, Gln88, Ser88, Thr160, Gly214, and Gly219 were prominently involved in van der Waals interactions. A similar competitive hydrogen-bonding interaction between ligands and proteins was reported in a previous paper [54]. LSI6 is a homolog of LSI1, so docking interactions are expected to be similar. This study selected phosphoric acid (H_3PO_4) as the positive control because of its structural and molecular weight similarities to silicic acid, suggesting its potential to bind to the transporter protein. Molecular docking results showed that H_3PO_4 had binding affinities of -3.9 and -4.0 kcal mol^{-1}, comparable to those of the studied ligand (Table 5). On the other hand, NaCl was chosen as the negative control, showing lower binding affinities (-1.9 and -1.8 kcal mol^{-1}) than those of both LSI1 and LSI6 transporters.

The amino acid residues observed in this study are suggested to form part of the transporter's binding site, which is likely crucial for ligand interaction. Three selectivity filter (SF) residues for both LSI1 and LSI6 interact with $Si(OH)_4$: Ser207, Gly216, and Arg222 for LSI1; and Ser210 and Gly218 for LSI6. The molecular docking results for LSI1 and LSI6 are consistent with the predicted location of $Si(OH)_4$ in site 2 (Si2) from the previous study [19]. These results indicate that LSI1 and LSI6 exhibit strong selectivity for $Si(OH)_4$ during transport across the root (LSI1) and node I (LSI6). A previous study also showed that SF residues are unique to the NIP III family, as they provide four oxygen atoms in the channel that allow interaction (hydrogen acceptor and donor) with the hydroxyl group in $Si(OH)_4$ [21]. In the silica selectivity filter, the TGSGR residues include three small residues compared with those of other aquaporins. Gly and Ser are small, simple residues that provide more space for silica to pass through the tunnel. The small size of the residues can contribute to ligand-protein interactions via hydrogen bonding [55].

Molecular docking results suggest that the ligand $Si(OH)_4$ can interact with all LSI transporter proteins via hydrogen bonds and Van der Waals interactions. These two types of interactions (between the ligand and the amino acid), along with the binding energy (ΔG) and the inhibition constant (Ki), are fundamental parameters for determining the interaction's affinity [56]. More negative binding free energy (ΔG) values indicate higher binding affinity, suggesting a more stable interaction between the ligand and the protein [57]. In this study, the binding affinity results for interactions between $Si(OH)_4$ and all LSI transporter proteins show minimal differences, ranging from -3.8 to -4.0 kcal mol^{-1} (Table 4). The low binding affinity indicates a negative free energy of binding (ΔG) and a lower inhibition constant (Ki). These findings suggest that $Si(OH)_4$ does not bind tightly to the active binding sites of LSIs during transport in rice plants. Additionally, van der Waals interactions enhance the complex's stability [58].

The findings for the positive and negative controls provide valuable insights into the specificity of these silica transporter proteins. The positive control, H_3PO_4, shows a binding affinity for $Si(OH)_4$ that is similar, suggesting that H_3PO_4 may compete with $Si(OH)_4$ for binding to LSIs. Both H_3PO_4 and $Si(OH)_4$ exhibit tetrahedral geometry and similar molecular weights [59]. These similarities suggest that LSIs might facilitate H_3PO_4 uptake during transport. Higher H_3PO_4 uptake can reduce $Si(OH)_4$ accumulation in the upper parts of plants. This can disrupt the strength of plant cell walls, which is essential for enhancing plants' resistance to biotic and abiotic stresses.

Table 4. Molecular interactions and docking parameters between the Si(OH)4 ligand and the silica influx transporter proteins (LSI1 and LSI6)

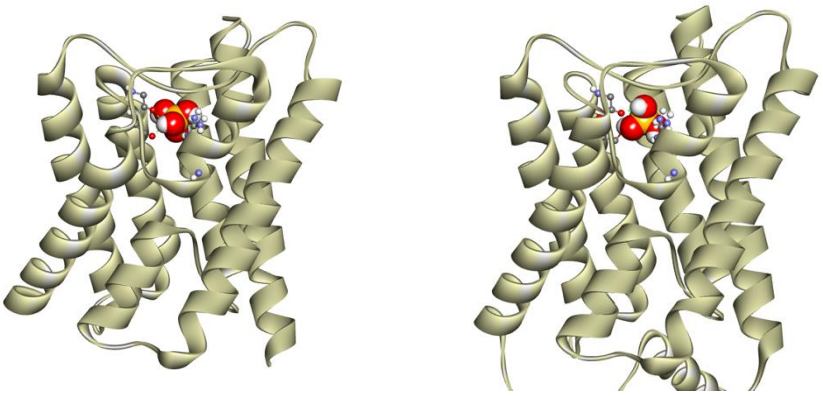
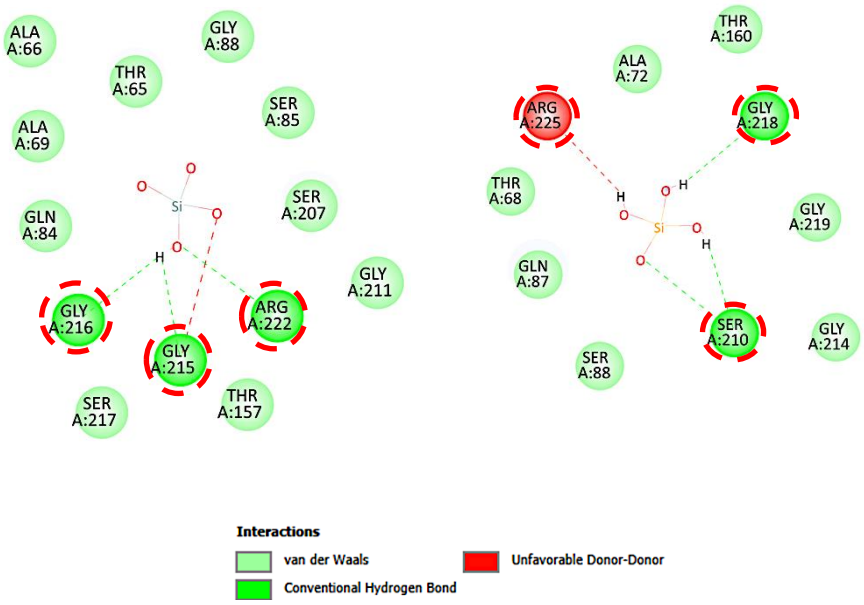
Molecular Docking	Protein	
	LSI1	**LSI6**
3D		
2D		
Binding affinity	-3.8	-4.0
No. H-bond	4	4
No. Van der Waals interaction	10	7

Table 5. Binding affinities of controlled ligands to the silica transporter proteins (LSI1 and LSI6)

Proteins	Binding Affinity (kcal mol^{-1})	
	Positive Control: Phosphoric Acid (H_3PO_4)	Negative Control: Sodium Chloride (NaCl)
LSI1	-3.9	-1.9
LSI6	-4.0	-1.8

On the other hand, NaCl (negative control) was used because of its simpler structure and larger size compared to $Si(OH)_4$. This study reports a much lower binding affinity than that of $Si(OH)_4$. These results confirm that the other molecule, with a different structure and larger than $Si(OH)_4$, does not interact strongly with the transporter and will be inhibited from entering the tunnel. In addition, the aquaporin family allows only small, selective molecules to pass [60, 61]. These findings support the idea that the silica transporter protein can specifically bind $Si(OH)_4$ and related molecules.

LSI6 plays a key role in enhancing Si uptake from the enlarged vascular bundle (EVB) into the diffuse vascular bundle (DVB) for distribution in rice husks. In rice plants, the LSI6 transporter has been identified on the polar side of the xylem transfer cell (XTC) within the enlarged vascular bundle (EVB) at node I. Moreover, XTCs are characterized by a folded plasma membrane with increased surface area, suggesting that more LSI6 protein is embedded in the membrane and involved in $Si(OH)_{4\ uptake}$. This suggestion is supported by previous research, which reported that Lsi6 gene knockout reduces Si deposition in the panicle but increases it in the flag leaf [62-65]. In these computational studies, the weak interaction between $Si(OH)_4$ and the LSI6 transporter is modeled as a transient binding event, indicating it is brief and fast. Thus, the high surface area of XTCs and the transient interaction facilitate efficient transport of $Si(OH)_4$ and contribute to the high accumulation of Si in rice husks.

Conclusion

In soil, silica nanoparticles (SiNPs) primarily exist as ortho-silicic acid ($Si(OH)_4$). In rice plants, $Si(OH)_4$ is absorbed by the roots and transported throughout the plant via four transporter proteins: LSI1, LSI2, LSI3, and LSI6. Among these, LSI6 facilitates the influx of $Si(OH)_4$. This study focused on characterizing the modeled structure of LSI6 and its molecular interaction with $Si(OH)_4$. The predicted LSI6 model, selected based on validation scores, revealed a hydrophobic transmembrane structure containing an NPA domain and a silica selectivity filter residue (TGSGR). The predicted binding site forms a tunnel-like pocket that likely plays a key role in $Si(OH)_4$ transport. Molecular docking results indicated low binding affinity between $Si(OH)_4$ and LSI6, suggesting a transient interaction during transport. Hydrogen bonding and van der Waals interactions were identified as key contributors to this interaction, particularly at the selectivity filter region. This fast, weak binding may facilitate the efficient transport of many $Si(OH)_4$ molecules through the transporter. Overall, this in silico study provides valuable insights into the molecular basis of $Si(OH)_4$ transport via the LSI6 protein in rice.

Future studies could use multiple molecular docking software packages to provide a broader, more reliable perspective on the interactions between $Si(OH)_4$ and LSIs, as different tools employ distinct algorithms and scoring functions. Comparative docking results may further strengthen the interpretation of protein-ligand interactions. In addition, comparative studies of other silicon transporters, such as LSI2 and LSI3, would contribute to a more comprehensive understanding of silicon transport in rice. Finally, molecular dynamics (MD) simulations could be included in future work to investigate further the stability and time-independence of the LSI6-$Si(OH)_4$ complex as well as the possible transport of $Si(OH)_4$ through the LSI6 tunnel under physiological conditions.

Acknowledgement

This project is funded by the government of Malaysia for a research grant under the Long-Term Research Grant Scheme (LRGS) from the Ministry of Higher Education Malaysia for the research program "Development of Climate Ready Rice for Sustaining Food Security in Malaysia" under grant No: LRGS/1/2019/UPM/01/2.

References

1. Abbass, K., Qasim, M. Z., Song, H., Murshed, M., Mahmood, H. and Younis, I. (2022). A review of the global climate change impacts, adaptation, and sustainable mitigation measures. *Environmental Science and Pollution Research,* 29(28): 42539–42559.
2. Anupama, A., Bhugra, S., Lall, B., Chaudhury, S. and Chugh, A. (2019). Morphological, transcriptomic and proteomic responses of contrasting rice genotypes towards drought stress. *Environmental and Experimental Botany,* 166: 103795.
3. Kumar, S., Dwivedi, S. K., Basu, S., Kumar, G., Mishra, J. S., Koley, T. K., Rao, K. K., Choudhary, A. K., Mondal, S., Kumar, S.,

Bhakta, N., Bhatt, B. P., Paul, R. K. and Kumar, A. (2020). Anatomical, agro-morphological and physiological changes in rice under cumulative a nd stage specific drought conditions prevailed in eastern region of India. *Field Crops Research*, 245: 107658.

4. Saha, S., Begum, H. and Nasrin, S. (2019). Effects of drought stress on growth and accumulation of proline in five rice varieties (*Oryza Sativa* L.). *Journal of the Asiatic Society,* 45: 241–247.
5. Larkunthod, P., Boonlakhorn, J., Pansarakham, P., Pongdontri, P., Thongbai, P. and Theerakulpisut, P. (2022). Synthesis and charact erization of silica nanoparticles from rice husk and their effects on physiology of rice under salt stress. *Chilean Journal of Agricultural Research* 82(3): 412–425.
6. Lavinsky, A. O., Detmann, K. C., Reis, J. V., Áv ila, R. T., Sanglard, M. L., Pereira, L. F., Sanglard, L. M. V. P., Rodrigues, F. A., Araújo, W. L. and DaMatta, F. M. (2016). Silicon improves rice grain yield and photosynthesis specifically when supplied during the reproductive growth stage. *Journal of Plant Physiology*, 206, 125–132.
7. Greger, M., Landberg, T. and Vaculík, M. (2018). Silicon influences soil availability and accumulation of mineral nutrients in various plant species. *Plants,* 7(2): 41.
8. Ng, L. C., Adila, Z. N., Shahrul Hafiz, E. M. and Aziz, A. (2021). Foliar spray of silicon enhances resistance against pyricularia oryzae by triggering phytoalexin responds in aerobic rice. *European Journal of Plant Pathology,* 159(3): 6 73–683.
9. Sharma, A., Vishwakarma, K., Singh, N. K., Prakash, V., Ramawat, N., Prasad, R., Ramawat, N., Prasad, R., Sahi, S., Singh, V. P., Tripathi, D. K. and Sharma, S. (2022). Synergistic action of silicon nanoparticles and indole acetic acid in all eviation of chromium (CrVI) toxicity in *Oryza sativa* seedlings. *Journal of Biotechnology,* 343: 71–82.
10. Seleiman, M. F., Al-Selwey, W. A., Ibrahim, A. A., Shady, M. and Alsadon, A. A. (2023). Foliar applications of ZnO and SiO_2 nano particles mitigate water deficit and enhance potato yield and quality traits. *Agronomy,* 13(2): 466.
11. Tran, T. L. C., Guirguis, A., Jeyachandran, T., Wang, Y. and Cahill, D. M. (2023). Mesoporous silica nanoparticle-induced drought tolerance in *Arabidopsis thaliana* grown under in vitro conditions. *Functional Plant Biology,* 50(11): 88 9–900.
12. Elshayb, O. M., Nada, A. M., Ibrahim, H. M., Amin, H. E. and Atta, A. M. (2021). Application of silica nanoparticles for improving growth, yield, and enzymatic antioxidant for the hybrid rice EHR1 growing under water regime conditio ns. *Materials,* 14(5): 1150.
13. Du, J., Liu, B., Zhao, T., Xu, X., Lin, H., Ji, Y., Li, Y., Li, Z., Lu, C., Li, P., Zhao, H., Li, Y., Yin, Z. and Ding, X. (2022). Silica nanoparticles prot ect rice against biotic and abiotic stresses. *Journal of Nanobiotechnology,* 20(1): 1–18.
14. Behboudi, F., Sarvestani, Z. T., Kassaee, M. Z., Modares, S. A. M. and Sorooshzadeh, A. (2018). Improving growth and yield of wheat under drought stress via application of SiO_2 nano particles, 20(7): 1479–1492.
15. Ismail, L. M., Soliman, M. I., Abd El-Aziz, M. H. and Abdel-Aziz, H. M. M. (2022). Impact of silica ions and nano silica on growth and produc tivity of pea plants under salinity stress. *Plants,* 11(4): 494.
16. Rao, G. B. and Susmitha, P. (2017). Silicon uptake, transportation and accumulation in rice. *Journal of Pharmacognosy Phytochemistry*, 6(6): 290–293.
17. Ali, A., Mir, G. J., Ayaz, A., Maqbool, I., Ahmad, S. B., Mushtaq, S., Khan, A., Mir, T. M. and Rehman, M. U. (2023). In silico analysis and molecular docking studies of natural compounds of *Withania somnifera* against bovine NLRP9. *Journal of Molecular Modeling*, 29(6): 171.
18. Salmaso, V. and Moro, S. (2018). Bridging molecular docking to molecular dynamics in exploring ligand-protein recognition process: An overview. *Frontiers in Pharmacology*, 9: 923.
19. Saitoh, Y., Mitani-Ueno, N., Saito, K., Matsuki, K., Huang, S., Yang, L., Yamaji, N., Ishikita, H., Shen, J. R., Ma, J. F. and Suga, M. (2021). Structural basis for high selectivity of a rice silicon channel Lsi1. *Nature Communications*, 12(1): 6236.
20. Saitoh, Y. and Suga, M. (2022). Structure and function of a silicic acid channel Lsi1. *Frontiers in Plant Science,* 13: 982068.
21. van den Berg, B., Pedebos, C., Bolla, J. R., Robinson, C. V., Baslé, A. and Khalid, S. (2021). Structural basis for silicic acid uptake by higher plants. *Journal of Molecular Biology,* 433 (21): 167226.
22. Mundada, P. S., Barvkar, V. T., Umdale, S. D., Anil Kumar, S., Nikam, T. D. and Ahire, M. L. (2021). Characterization of influx and efflux silicon transporters and understanding their role in the osmotic stress tolerance in finger millet (*Eleusine coracana* (L.) Gaertn.). *Plant Physiology and Biochemistry,* 162: 677–689.
23. Colovos, C. and Yeates, T. O. (1993). Verification of protein structures: patterns of non bonded atomic interactions. *Protein Science*, 2(9): 1511–1519.
24. Ramachandran, G. N., Ramakrishnan, C. and Sa sisekharan, V. (1963). Stereochemistry of poly peptide chain configurations. *Journal of*

Molecular Biology, 7(1): 95–99.

25. Madeira, F., Madhusoodanan, N., Lee, J., Eusebi, A., Niewielska, A., Tivey, A. R. N., Lopez, R. and Butcher, S. (2024). The EMBL-E BI job dispatcher sequence analysis tools frame work in 2024. *Nucleic Acids Research,* 52(1): 52 1–525.
26. Gasteiger, E., Hoogland, C., Gattiker, A., Duvau d, S., Wilkins, M. R., Appel, R. D. and Bairoch, A. (2005). Protein identification and analysis too ls on the ExPASy server. The Proteomics Protocols Handbook, Totowa, New Jersey: pp. 5 71–607.
27. Jones, G., Jindal, A., Ghani, U., Kotelnikov, S., Egbert, M., Hashemi, N., Vajda, S., Padhorny, D. and Kozakov, D. (2022). Elucidation of protein function using computational docking and hotspot analysis by ClusPro and FTMap. *Acta Crystallographica Section D Structural Biology,* 78(6): 690–697.
28. Schrödinger, L. and DeLano, W. (2020). PyMOL (Version 2.5.2) [Computer software].
29. Pravda, L., Sehnal, D., Toušek, D., Navrátilová, V., Bazgier, V., Berka, K., Berka, K., Svobodová Vařeková, R., Koča, J. and Otyepka, M. (2018). MOLEonline: a web-based tool for analyzing channels, tunnels and pores (2018 update). *Nucleic Acids Research,* 46(1): 368–373.
30. Rangisetty, P. T., Kilaparthi, A., Akula, S., Bhardwaj, M. and Singh, S. (2023). RSAD2: An exclusive target protein for zika virus comparative modeling, characterization, energy minimization and stabilization. *International Journal of Health Sciences,* 17(1): 12-17.
31. Eberhardt, J., Santos-Martins, D., Tillack, A. F. and Forli, S. (2021). AutoDock Vina 1.2.0: New docking methods, expanded force field, and python bindings. *Journal of Chemical Information and Modeling,* 61(8): 3891–3898.
32. Larbaoui, B. and Menad, R. (2024). Single-click molecular docking via SwiftDock: A new virtual screening tool using AutoDock4. *Computational and Structural Biotechnology Reports*, 1: 10001 7.
33. Baroroh, U., Muscifa, Z. S., Destiarani, W., Rohmatullah, F. G. and Yusuf, M. (2023). Molecular interaction analysis and visualization of protein-ligand docking using Biovia Discovery Studio visualizer. *Indonesian Journal of Computational Biology,* 2(1): 22.
34. Jumper, J., Evans, R., Pritzel, A., Green, T., Figurnov, M., Ronneberger, O., Tunyasuvunakool, K., Bates, R., Žídek, A., Potapenko, A., Bridgland, A., Meyer, C., Kohl, S. A. A., Ballard, A. J., Cowie, A., Romera-Paredes, B., Nikolov, S., Jain, R., Adler, J., Back, T., Peterson, S., Reiman, D., Clancy, E., Zienliski, M., Steinegger, M., Pacholska, M., Berghammer, T., Bodenstein, S., Silver, D., Vinyals, O., Senior, A. W., Kavukcuoglu, K., Kohli, P. and Hassabis, D. (2021). Highly accura te protein structure prediction with AlphaFold. *Nature,* 596(7873): 583–589.
35. Baek, M., DiMaio, F., Anishchenko, I., Dauparas, J., Ovchinnikov, S., Lee, G. R., Wang, J., Cong, Q., Kinch, L. N., Schaeffer, R. D., Millán, C., Park, H., Adams, C., Glassman, C. R., DeGiovanni, A., Pereira, J. H., Rodrigues, A. V., Van Dijk, A. A., Ebrecht, A. C., Opperman, D. J., Sagmeister, T., Buhlheller, C., Pavkov-Keller, T., Rathinaswamy, M. K., Dalwadi, U., Yip, C. K., Grishin, N. V., Adams, P. D., Read, R. J. and Baker, D. (2021). Accurate prediction of protein structures and interactions using a three-track neural network. *Science,* 373(6557): 871–876. \
36. Waterhouse, A., Bertoni, M., Bienert, S., Studer, G., Tauriello, G., Gumienny, R., Heer, F. T., de Beer, T. A. P., Rempfer, C., Bordoli, L., Lepore, R. and Schwede, T. (2018). SWISS-MODEL: Homology modelling of protein struct ures and complexes. *Nucleic Acids Research,* 46 (1): 296–303.
37. Burley, S. K., Bhikadiya, C., Bi, C., Bittrich, S., Chao, H., Chen, L., Craig, P. A., Crichlow, G. V., Dalenberg, K., Duarte, J. M., Dutta, S., Fayazi, M., Feng, Z., Flatt, J. W., Ganesan, S., Ghosh, S., Goodsell, D. S., Green, R. K., Guranovic, V., Henry, J., Hudson, B. P., Khokhriakov, I., Lawson, C. L., Liang, Y. Lowe, R., Peisach, E., Persikova, I., Piehl, D. W., Rose, Y., Sali, A., Segura, J., Sekharan, M., Shao, C., Vallat, B., Voight, M., Webb, B., Westbrook, J. D., Whestone, S. Young, J. Y., Zalesky, A. and Zard ecki, C. (2023). RCSB Protein Data Bank (RCS B.org): Delivery of experimentally-determined PDB structures alongside one million computed structure models of proteins from artificial intelligence/machine learning. *Nucleic Acids Research,* 51(1): 488–508.
38. Coudert, E., Gehant, S., De Castro, E., Pozzato, M., Baratin D., Neto, T., Sigrist, C. J. A., Redaschi, N., Bridge, A. and The Uni Prot Consortium. (2023). Annotation of Biologic ally Relevant Ligands in UniProtKB using ChEBI. *Bioinformatics,* 39(1).
39. Kim, S., Chen, J., Cheng, T., Gindulyte, A., He, J., He, S., Li, Q., Shoemaker, B. A., Thiessen, P. A., Yu, B., Zaslavsky, L., Zhang, J. and Bolton, E. E. (2023). PubChem 2023 update. *Nucleic Acids Research,* 51(1): 1373–1380.
40. Boittier, E. D., Tang, Y. Y., Buckley, M. E., Schuurs, Z. P., Richard, D. J. and Gandhi, N. S. (2020). Assessing molecular docking tools to guide targeted drug discovery of CD38 inhibitors. *International Journal of Molecular Sciences,* 21(15): 5183.
41. Azam, S. S. and Abbasi, S. W. (2013). Molecular docking studies for the identification of novel melatoninergic inhibitors for acetylsero

tonin-o-methyltransferase using different dockin g routines. *Theoretical Biology and Medical Modelling,* 10(1): 63.

42. Debnath, P., Khan, U. and Khan, Md. S. (2022). Characterization and structural prediction of proteins in SARS-CoV-2 Bangladeshi variant through bioinformatics. *Microbiology Insights,* 15: 11786361221115595.
43. Santhoshkumar, R. and Yusuf, A. (2020). In silico structural modeling and analysis of physic ochemical properties of curcumin synthase (CURS1, CURS2, and CURS3) proteins of *Curcuma longa*. *Journal of Genetic Engineering and Biotechnology,* 18(1): 24.
44. Han, Y., Lin, Z., Zhou, J., Yun, G., Guo, R., Richardson, J. J. and Caruso, F. (2020). Polyphenol‐mediated assembly of proteins for engineering functional materials. *Angewandte Chemie International Edition,* 59(36): 15618–15625.
45. Kyte, J. and Doolittle, R. F. (1982). A simple method for displaying the hydropathic character of a protein. *Journal of Molecular Biology,* 157 (1): 105–132.
46. Bagag, A., Jault, J.-M., Sidahmed-Adrar, N., Réfrégiers, M., Giuliani, A. and Le Naour, F. (2013). Characterization of hydrophobic peptide s in the presence of detergent by photoionization mass spectrometry. *PLoS ONE,* 8(11): e79033.
47. Fillería, S. G., Nardo, A. E., Paulino, M. and Tironi, V. (2021). Peptides derived from the gast rointestinal digestion of Amaranth 11S Globulin : Structure and antioxidant functionality. *Food Chemistry: Molecular Sciences,* 3: 100053.
48. The UniProt Consortium. (2023). UniProt: The Universal Protein Knowledgebase in 2023. *Nucleic Acids Research,* 51(1): 523–531.
49. Carugo, O. (2023). pLDDT values in Alphafold2 protein models are unrelated to globular protein local flexibility. *Crystals,* 13(11): 1560.
50. Bertoni, M., Kiefer, F., Biasini, M., Bordoli, L. and Schwede, T. (2017). Modeling protein quate rnary structure of homo- and hetero-oligomers beyond binary interactions by homology. *Scientific Reports,* 7(1): 10480.
51. Ngan, C.-H., Hall, D. R., Zerbe, B., Grove, L. E. , Kozakov, D. and Vajda, S. (2012). FTSite: High accuracy detection of ligand binding sites on unbound protein structures. *Bioinformatics,* 28(2): 286–287.
52. David, O. A., Labulo, A. H., Hassan, I., Olawuni, I., Oseghale, C. O., Terna, A. D., Ajayi, O. O., Ayegbusi, S. A. and Owolabi, M. O. (2024). Complexation and immobilization of arsenic in maize using green synthesized silicon nanoparticles (SiNPs). *Scientific Reports,* 14(1): 6176.
53. Raza, M. A. S., Zulfiqar, B., Iqbal, R., Muzamil, M. N., Aslam, M. U., Muhammad, F., Amin, J., Aslam, H. M. U., Ibrahim, M. A., Uzair, M. and Habib-ur-Rahman, M. (2023). Morpho-physiological and biochemical response of wheat to various treatments of silicon nano-particles under drought stress conditions. *Scientific Reports,* 13(1): 2700.
54. Osman, U. M., Silvarajoo, S., Noor Hassim, M. F., Arshad, S., Anizaim, A. H. and Abdul Razak, F. I. (2021). Synthesis, X-ray structure, Hirshfeld surface analysis, DFT calculations, and molecular docking studies of nickel(II) complex with thiosemicarbazone derivative. *Bio inorganic Chemistry and Applications*, 2021(1): 5536902.
55. Pilus, N. S. M., Muhamad, A., Shahidan, M. A. and Yusof, N. Y. M. (2022). Potential of epidermal growth factor-like peptide from the sea cucumber *Stichopus horrens* to increase the growth of human cells: in silico molecular docki ng approach. *Marine Drugs,* 20(10): 596.
56. Du, X., Li, Y., Xia, Y. L., Ai, S. M., Liang, J., Sang, P., Ji, X. L. and Liu, S. Q. (2016). Insights into protein–ligand interactions: Mechanisms, models, and methods. *International Journal of Molecular Sciences,* 17(2): 144.
57. Jia, C. S., Wang, Y. T., Wei, L. S., Wang, C. W., Peng, X. L. and Zhang, L. H. (2019). Predict-ions of entropy and Gibbs energy for carbonyl s ulfide. *ACS Omega,* 4(22): 20000–20004.
58. Iqbal, D., Alsaweed, M., Jamal, Q. M. S., Asad, R. M., Rizvi, S. M. D., Rizvi, M. R., Albadrani, H. M., Hamed, M., Jahan, S. and Alyenbaawi, H. (2023). Pharmacophore-based screening, molecular docking, and dynamic simulation of fungal metabolites as inhibitors of multi-targets in neurodegenerative disorders. *Biomolecules,* 13(11): 1613.
59. Persson, I., Trublet, M. and Klysubun, W. (2018). Structure determination of phosphoric acid and phosphate ions in aqueous solution using EXAFS spectroscopy and large angle X-ray scattering. *The Journal of Physical Chemistry A*, 122(37): 7413–7420.
60. Zhang, Y., Fei, S., Xu, Y., He, Y., Zhu, Z. and Liu, Y. (2022). The structure, function and expression analysis of the nodulin 26-like intrinsic protein subfamily of plant aquaporins in tomato. *Scientific Reports,* 12(1): 9180.
61. Duan, Y., Su, Y., Han, R., Sun, H. and Gong, H. (2022). Nodulin 26-like Intrinsic Protein CsNIP 2;2 is a silicon influx transporter in *Cucumis sativus* L. *Journal of Integrative Agriculture*, 21 (3): 685–696.
62. Jian, F. M., Tamai, K., Yamaji, N., Mitani, N., Konishi, S., Katsuhara, M., Ishiguro, M., Murata, Y. and Yano, M. (2006). A silicon transporter in rice. *Nature,* 440(7084): 688–691.
63. Ma, J. F., Yamaji, N., Mitani, N., Tamai, K., Konishi, S., Fujiwara, T., Katsuhara, M. and Yano, M. (2007). An efflux transporter of silicon in rice. *Nature,* 448(7150): 209–212.

64. Yamaji, N., Mitatni, N. and Ma, J. F. (2008). A transporter regulating silicon distribution in rice shoots. *The Plant Cell,* 20(5): 1381–1389.
65. Yamaji, N., Sakurai, G., Mitani-Ueno, N. and Ma, J. F. (2015). Orchestration of three transport ers and distinct vascular structures in node for in tervascular transfer of silicon in rice. *Proceeding of the National Academy of Sciences of the United States of America,* 112(36): 11401–11406.